ISSN 1063-7761, Journal of Experimental and Theoretical Physics, 2006, Vol. 102, No. 2, pp. 234–247. © Pleiades Publishing, Inc., 2006
Original Russian Text © V.V. Val'kov, V.A. Mitskan, G.A. Petrakovskiĭ, 2006, published in Zhurnal Éksperimental'noĭ i Teoreticheskoĭ Fiziki, 2006, Vol. 129, No. 2, pp. 268–282.

ORDER, DISORDER, AND PHASE TRANSITIONS IN CONDENSED SYSTEMS

The Magnetoelastic Mechanism of Singlet Phase Formation in a Two-Dimensional Quantum Antiferromagnet

V. V. Val'kov[a,b,c,*], V. A. Mitskan[a,b], and G. A. Petrakovskiĭ[a,b]

[a] *Institute of Physics, Siberian Division, Russian Academy of Sciences, Krasnoyarsk, 660036 Russia*
[b] *Krasnoyarsk State Technical University, Krasnoyarsk, 660074 Russia*
[c] *Krasnoyarsk State University, Krasnoyarsk, 660075 Russia*
**e-mail: vvv@iph.krasn.ru*

Received May 30, 2005

Abstract—A model describing the second-order phase transition with respect to the magnetoelastic coupling parameter from the antiferromagnetic (AFM) to the singlet state in a two-dimensional quantum magnet on a square lattice is proposed. The spectrum of elementary excitations in the singlet and AFM phases is calculated using an atomic representation, and the evolution of transverse and longitudinal branches of this spectrum is studied in the vicinity of the transition point. It is established that the AFM to singlet phase transition is related to softening of the longitudinal branch of oscillations. In the singlet phase, the gap plays the role of a parameter characterizing the distance to the phase transition point. It is shown that the spectrum of transverse oscillations in the AFM phase corresponds to the Goldstone boson. Based on an analysis of the stability of the spectrum of elementary excitations, a phase diagram is constructed that determines the regions of the existence of phases with plaquette-deformed lattices.

PACS numbers: 71.27.+a, 74.90.+n, 75.10.Lp

DOI: 10.1134/S106377610602004X

1. INTRODUCTION

In recent years, much attention has been devoted to investigations into the properties of quantum magnets representing the so-called spin-gap systems, in which an energy gap appears for certain reasons in the spectrum of elementary excitations. Examples of such systems are offered by the spin-Peierls magnet $CuGeO_3$ [1, 2], two-dimensional (2D) Heisenberg magnet CaV_4O_9 [3], and 2D spin systems such as $SrCu_2(BO_3)_2$ [4] and $(C_4H_{12}N_2)Cu_2Cl_6$ [5].

As is well known, the energy spectrum of exchange-coupled spin pairs (dimers) with the spin $S = 1/2$ comprises the singlet and triplet states separated by an energy gap that is determined by the value of the coupling parameter. In the case of systems with antiferromagnetic (AFM) coupling of spin moments, the singlet state corresponds to the lower energy level. At the same time, the spectrum of magnetic excitations of a homogeneous AFM chain is gapless. For these reasons, the magnetic susceptibilities of systems of the two types exhibit different temperature dependences: the susceptibility of a dimeric magnet vanishes as $T \longrightarrow 0$, whereas that of the homogeneous AFM chain at $T = 0$ is nonzero. In a "dimerized" chain with the coupling parameters J and J^*, the spectrum of magnetic excitations exhibits an energy gap $\Delta \sim |J - J^*|$ and the magnetic susceptibility decays according to an exponential law for $T \longrightarrow 0$ [6]. In such cases, magnetoelastic coupling plays a key role in the singlet state formation.

Evidently, an analogous situation can be expected to occur in a 2D spin system featuring AFM exchange interactions. Indeed, a sharp decrease in the susceptibility with decreasing temperature has been observed in many quasi-2D quantum magnets (see, e.g., [4, 5, 7, 8]). One obvious reason for this behavior of the magnetic susceptibility is the special energy structure of spin clusters in such systems. In particular, in systems with square lattices, an important role is played by the character of the energy spectrum of a four-spin square plaquette. In the case of AFM coupling, the intrinsic energy levels are such that the singlet spin state corresponds to a lower energy level [9], whereas the other levels are separated by an energy gap that is determined by the magnitude of the exchange interaction. For this reason, the magnetic susceptibility of a separate plaquette vanishes as $T \longrightarrow 0$. On the other hand, the spectrum of spin-wave excitations of a 2D square lattice is free of energy gaps and the corresponding magnetic susceptibility at $T = 0$ is nonzero.

In this context, it was of interest to study the conditions of formation of the ground singlet state with a gapped energy spectrum of elementary excitations in 2D quantum magnets. In such systems, the mechanism of the singlet phase formation is related to the possibility for a set of spins to form "clusters" (this situation probably takes place in $(C_4H_{12}N_2)Cu_2Cl_6$ [5]), rather

than to a specific topology of exchange bonds (as, e.g., in $SrCu_2(BO_3)_2$ [4]). Here, by the cluster, we imply a group of spins in which the character of mutual interactions is substantially distinct from that of the interactions between spins belonging to different groups. Below we present the results of an analysis of this problem in a simplified variant, whereby spin clusters have the form of plaquettes of a 2D square lattice.

The paper is organized as follows. In Section 2, we consider the influence of plaquette deformation in a square lattice on the ground state of a 2D quantum magnet. In Section 3, the Hubbard operator technique is used to construct a plaquette representation that allows all the intraplaquette quantum fluctuations to be taken into consideration. Section 4 describes the derivation of a dispersion equation for the spectrum of elementary excitations in the plaquette-deformed singlet phase. Section 5 presents a solution to the dispersion equation in a low-temperature phase and gives an analysis of the modification of the gapped spectrum on approaching the point of transition to the magnetic phase. In Section 6, we construct the plaquette representation with allowance for the self-consistent field effects. Section 7 is devoted to calculations of the spectrum of collective excitations in the AFM phase and to an analysis of the evolution of this spectrum in the vicinity of a transition to the singlet phase. Section 8 summarizes the main results.

2. PLAQUETTE DEFORMATION OF A 2D QUANTUM MAGNET

First, let us qualitatively analyze the influence of magnetoelastic coupling (MEC) on the ground state of a 2D quantum magnet in the presence of plaquette deformation and formulate the corresponding model concepts.

We assume that, prior to the MEC onset, the spin moments with $S = 1/2$ occur at the nodes of the ideal square lattice with the parameter a_0. The interaction between these spins is described in terms of the Heisenberg Hamiltonian with two exchange parameters, $I > 0$ and $J > 0$:

$$H = \frac{1}{2}\sum_f \sum_{\delta_1} I(\mathbf{S}_f \mathbf{S}_{f+\delta_1}) + \frac{1}{2}\sum_f \sum_{\delta_2} J(\mathbf{S}_f \mathbf{S}_{f+\delta_2}), \quad (1)$$

where $\mathbf{S}_f$ is the vector operator corresponding to a spin moment occurring at the fth node. The first and second terms on the right-hand side of Eq. (1) refer to the exchange interactions between spins that are the nearest and next-to-nearest neighbors. The signs at I and J are selected to establish AFM coupling of the spins involved in the interaction.

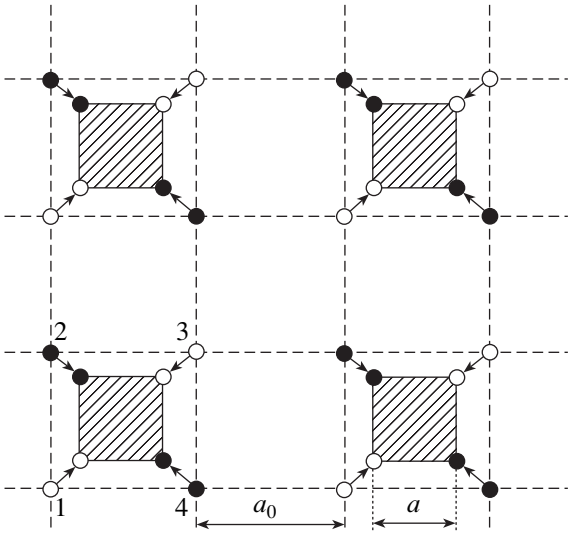

Fig. 1. Schematic diagram of the plaquette deformation of a square lattice (see text for explanations).

With allowance for the MEC, the minimum free energy is attained in a deformed state of the lattice. This situation takes place, for example, in systems where the exchange integral is a linear function of the relative displacements of spins. Then, the exchange energy gain (which also linearly depends on the relative displacements) exceeds the quadratic loss in the elastic energy. This mechanism of magnetostriction is well known and frequently encountered in magnetically ordered substances [10].

In systems with developed quantum fluctuations, such as frustrated quasi-2D antiferromagnets, allowance for the MEC may lead to more radical changes. This is related primarily to the possibility of a change in the structure of the ground state in the spin subsystem. The mechanism of this modification is determined by a competition between the tendency toward "singletization" (at the expense of quantum fluctuations in frustrated low-dimensional antiferromagnets) and the opposite trend of retaining the spontaneously broken symmetry in the presence of a long-range magnetic order.

The aforementioned competition can be illustrated by variations in the exchange energy observed in the course of inhomogeneous plaquette deformation of a square lattice depicted in Fig. 1. In the initial state, the spin moments occur at the points of intersection of dashed lines and form the long-range AFM order, whereby the average value of the spin moment projection onto the quantization axis at the points denoted by open and filled circles are positive and negative, respectively. In a deformed state (with the spin moments shifted along the trajectories indicated by arrows), the spins are grouped into four-spin clusters (plaquettes) depicted by cross-hatched squares with a side length of

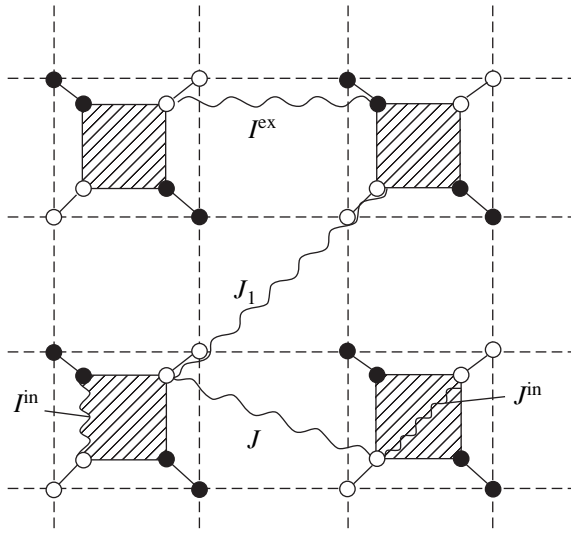

Fig. 2. Identification of the exchange interaction constants in a plaquette-deformed state (see text for explanations).

$a < a_0$. This kind of distortion of the initial lattice will be referred to below as plaquette deformation.

For the Néel phase with an undistorted lattice, the exchange energy per plaquette is $-2I$ (for simplicity, we restrict the consideration to a lattice where only the nearest neighbors are involved in the interaction). In the state where the spin moments of each plaquette form a spin singlet, the exchange energy per plaquette has the same value ($-2I$). These simple estimates show that the singlet phase is not preferred to the Néel state if the parameter I remains unchanged. As will be seen below, more rigorous calculations confirm this conclusion.

A different situation takes place if the plaquette deformation involves an increase in the intraplaquette ($I \longrightarrow I^{in} > I$) and a decrease in the interplaquette ($I \longrightarrow I^{ex} < I$) exchange integrals. In this case, the energy of the Néel phase is $E_N = -I^{in} - I^{ex}$, whereas that of the plaquette singlet phase is $E_S = -2I^{in}$. As can be seen, the magnetic energy gain upon breakage of the Néel state, $\Delta E = E_N - E_S = I^{in} - I^{ex}$, is positive and the singlet phase with plaquette deformation is preferred. This scenario of a plaquette singlet phase formation is an evident generalization to the 2D case of the aforementioned dimerization upon the spin-Peierls transition in a linear chain.

The above considerations outline a qualitative pattern and do not determine the conditions of a transition to the singlet phase. In order to study the problem in more detail, it is necessary to determine the spectrum of elementary excitations in the plaquette-deformed state of a frustrated 2D quantum magnet. Then, the stability of the singlet phase can be judged based on the criterion of positive definiteness of the energy spectrum. In addition, the knowledge of the energies of elementary excitations makes possible the calculation of the contribution due to quantum fluctuations to the observed characteristics of the system under consideration.

3. PLAQUETTE REPRESENTATION

In determining the spectrum of elementary excitations in a plaquette-deformed state, it is necessary to take into account the difference between the exchange integrals of spins belonging to the same and different plaquettes. At the point of breakage of the spin-ordered state, this difference can be so large that the intraplaquette interactions would provide for the main contribution to the Hamiltonian. Extrapolating this situation to the ultimate case, we arrive at a "plaquette" variant of perturbation theory, in which the operator describing an ensemble of plaquettes with exact allowance for all interactions in a separate plaquette is a zero-order Hamiltonian, while the interplaquette interactions play the role of perturbations.

In order to determine the form of a Hamiltonian in the representation corresponding to the plaquette variant of perturbation theory, let us assign all spin moments to plaquettes as depicted in Fig. 1. Each plaquette is characterized by a 2D vector $l = (nb, mb)$, where n and m are positive and negative integers and $b = 2a_0$ is the parameter of a new square lattice with the basis set including four spins. In this description, the spin moments acquire double numbering: l indicates the plaquette in which the spin moment occurs, and the other index refers to the node number in the plaquette. Accordingly, the vector operators of four spin moments in the lth plaquette are written as $\mathbf{S}_1(l)$, $\mathbf{S}_2(l)$, $\mathbf{S}_3(l)$, and $\mathbf{S}_4(l)$. The order of numbering nodes is indicated on the bottom left plaquette in Fig. 1.

Within the framework of the adopted distribution of spins over plaquettes, Hamiltonian (1) can be represented as

$$H = H_0 + H_{int}, \quad H_0 = \sum_l h_0(l), \tag{2}$$

where H_0 describes the noninteracting plaquettes or those interacting only by means of a self-consistent field (see below) and H_{int} describes the interplaquette interactions. The $h_0(l)$ operator is a one-plaquette Hamiltonian describing all the exchange interactions in the lth plaquette:

$$\begin{aligned} h_0(l) &= I^{in}[\mathbf{S}_1(l)\mathbf{S}_2(l) + \mathbf{S}_2(l)\mathbf{S}_3(l) \\ &\quad + \mathbf{S}_3(l)\mathbf{S}_4(l) + \mathbf{S}_4(l)\mathbf{S}_1(l)] \\ &\quad + J^{in}[\mathbf{S}_1(l)\mathbf{S}_3(l) + \mathbf{S}_2(l)\mathbf{S}_4(l)], \end{aligned} \tag{3}$$

where I^{in} and J^{in} are the exchange integrals of intraplaquette interactions (see Fig. 2). In the linear approx-

imation with respect to the displacements of spins, these integrals are defined as

$$I^{\text{in}} = (1 + k_1\delta)I, \quad J^{\text{in}} = (1 + k_2\delta)J,$$
$$I = I(r)|_{r = a_0}, \quad J = J(r)|_{r = \sqrt{2}a_0}, \tag{4}$$

where k_1 and k_2 are the parameters characterizing the relative rates of variation of the exchange integrals in response to the change in distances to the first and second coordination spheres:

$$k_1 = -\frac{a_0}{I}\left(\frac{\partial I(r)}{\partial r}\right)_{r = a_0},$$
$$k_2 = -\frac{\sqrt{2}a_0}{J}\left(\frac{\partial J(r)}{\partial r}\right)_{r = \sqrt{2}a_0}. \tag{5}$$

It will be assumed that the linear size a of a contracted plaquette can be expressed via the initial size a_0 using the relative linear deformation δ as $a = (1 - \delta)a_0$.

In order to construct the plaquette representation, let us introduce a basis set of the eigenstates of one-plaquette Hamiltonian (3). Solutions to the Schrödinger equation (to simplify writing, the plaquette index is temporarily omitted)

$$h_0|\Psi_{SM}\rangle = E|\Psi_{SM}\rangle \tag{6}$$

determine 16 eigenstates [9] with the functions $|\Psi_{SM}\rangle$ characterized by the total spin moment S and its projection M onto the quantization axis z. For brevity, below we present only the $|\Psi_{SM}\rangle$ functions belonging to different multiplets of a spin plaquette and having the maximum projection $M = S$ for a given spin moment S (i.e., the $|\Psi_{SS}\rangle$ functions). Then, one-plaquette wavefunctions with smaller M are obtained from $|\Psi_{SS}\rangle$ by applying (the appropriate number of times) the operator of reduction of the total moment projection ($S^- = s_1^- + s_2^- + s_3^- + s_4^-$) and multiplying by the corresponding normalization coefficient.

The lowest one-plaquette state with the minimum energy corresponds to the first spin singlet A_1,

$$|\Psi_{00}^{(1)}\rangle \equiv |\Phi_1\rangle = \frac{1}{2\sqrt{3}}\{|- - + +\rangle - 2|- + - +\rangle + |- + + -\rangle + |+ - - +\rangle - 2|+ - + -\rangle + |+ + - -\rangle\}, \tag{7}$$

and has the energy $E_1 = E(A_1) = -2I^{\text{in}} + J^{\text{in}}/2$. The next on the energy scale is the first spin triplet

$$T_1: \begin{cases} |\Psi_{1,1}^{(1)}\rangle \equiv |\Phi_2\rangle, & E_2 = E(T_1) = -I^{\text{in}} + J^{\text{in}}/2, \\ |\Psi_{1,0}^{(1)}\rangle \equiv |\Phi_3\rangle, & E_3 = E(T_1), \\ |\Psi_{1,-1}^{(1)}\rangle \equiv |\Phi_4\rangle, & E_4 = E(T_1). \end{cases} \tag{8}$$

The component of this triplet that corresponds to the maximum projection of the total spin moment is described by the function

$$|\Phi_2\rangle = \frac{1}{2}\{|- + + +\rangle - |+ - + +\rangle + |+ + - +\rangle - |+ + + -\rangle\}. \tag{9}$$

The second singlet state A_2 occurs above the first triplet, corresponds to the wavefunction

$$|\Psi_{00}^{(2)}\rangle \equiv |\Phi_5\rangle = \frac{1}{2}\{|- - + +\rangle - |- + + -\rangle - |+ - - +\rangle + |+ + - -\rangle\}, \tag{10}$$

and has the energy $E_5 = E(A_2) = -3J^{\text{in}}/2$. This level is followed by two degenerate spin triplets

$$T_2: \begin{cases} |\Psi_{1,1}^{(2)}\rangle \equiv |\Phi_6\rangle, \\ |\Psi_{1,0}^{(2)}\rangle \equiv |\Phi_7\rangle, \\ |\Psi_{1,-1}^{(2)}\rangle \equiv |\Phi_8\rangle, \end{cases}$$
$$T_3: \begin{cases} |\Psi_{1,1}^{(3)}\rangle \equiv |\Phi_9\rangle, \\ |\Psi_{1,0}^{(3)}\rangle \equiv |\Phi_{10}\rangle, \\ |\Psi_{1,-1}^{(3)}\rangle \equiv |\Phi_{11}\rangle, \end{cases} \tag{11}$$

with the energies $E(T_2) = E(T_3) \equiv E_p = -J^{\text{in}}/2$, $p = 6, 7, \ldots, 11$. The components of these triplets that correspond to the maximum projection $M = 1$ of the total spin moment are described by the functions

$$|\Phi_6\rangle = \frac{1}{\sqrt{2}}\{|- + + +\rangle - |+ + - +\rangle\},$$
$$|\Phi_9\rangle = \frac{1}{\sqrt{2}}\{|+ - + +\rangle - |+ + + -\rangle\}. \tag{12}$$

The maximum energy $E_p = E(D) = I^{\text{in}} + J^{\text{in}}/2$ ($p = 12, 13, \ldots, 16$) corresponds to the states of the spin quintet D with $S = 2$,

$$D: \{|\Psi_{2,2}\rangle \equiv |\Phi_{12}\rangle,\ |\Psi_{2,1}\rangle \equiv |\Phi_{13}\rangle,\ |\Psi_{2,0}\rangle \equiv |\Phi_{14}\rangle, |\Psi_{2,-1}\rangle \equiv |\Phi_{15}\rangle,\ |\Psi_{2,-2}\rangle \equiv |\Phi_{16}\rangle\},$$

in which two functions can be written in the adopted notation as

$$|\Psi_{2,2}\rangle \equiv |\Phi_{12}\rangle = |+ + + +\rangle,$$
$$|\Psi_{2,0}\rangle \equiv |\Phi_{14}\rangle = \frac{1}{\sqrt{6}}\{|- - + +\rangle + |- + - +\rangle + |- + + -\rangle + |+ + - -\rangle + |+ - - +\rangle + |+ - + -\rangle\}. \tag{13}$$

Here, $|\Psi_{2,2}\rangle$ is the function with the maximum projection of the total spin moment and $|\Psi_{2,0}\rangle$ is the function with the minimum projection that plays a substantial role in description of the spectral properties of the AFM phase. The above expressions for the energies of states show that the first singlet $|\Phi_1\rangle$ is the ground state for $I^{in} > J^{in}$ (otherwise, the second singlet $|\Phi_5\rangle$ is the ground state).

The basis set $\{|\Phi_q\rangle, q = 1, 2, \ldots, 16\}$ determines the Hilbert space in which the operators defined for each single plaquette are operative. Each operator can be expanded over the basis set operators that are conveniently represented by the Hubbard operators,

$$X^{pq} = |\Phi_p\rangle\langle\Phi_q|, \tag{14}$$

whose action on the $|\Phi_q\rangle$ state is defined by the relation

$$X^{pq}|\Phi_{q'}\rangle = \delta_{qq'}|\Phi_p\rangle. \tag{15}$$

Taking into account the properties of the Hubbard operators and restoring the plaquette index, the spin operators can be represented as

$$\begin{aligned} S_i^+(l) &= \sum_{pq}\gamma_i^\perp(p,q)X_l^{pq}, \\ S_i^-(l) &= \sum_{pq}\gamma_i^\perp(p,q)X_l^{qp}, \quad i = 1,2,3,4, \end{aligned} \tag{16}$$

where the representation parameters $\gamma_i^\perp(p, q)$ in short writing denote the matrix elements of the spin operator: $\gamma_i^\perp(p, q) = \langle\Phi_p|S_i^+|\Phi_q\rangle$. By the same token, we introduce a representation for the coordinate operators $S_i^z(l)$ as

$$\begin{aligned} S_i^z(l) &= \sum_{pq}\gamma_i^\parallel(p,q)X_l^{pq}, \\ \gamma_i^\parallel(p,q) &= \langle\Phi_p|S_i^z|\Phi_q\rangle. \end{aligned} \tag{17}$$

In terms of the Hubbard operators, Hamiltonian H_0 acquires the diagonal form:

$$H_0 = \sum_l\sum_{p=1}^{16}E_pX_l^{pp}. \tag{18}$$

Now let us express the perturbation Hamiltonian in the plaquette representation. Operator H_{int} describes the exchange coupling of spin moments belonging to different plaquettes and can be written as

$$\begin{aligned} H_{int} = \sum_l\{I^{ex}[&\mathbf{S}_4(l)\cdot\mathbf{S}_1(l+\Delta_x) \\ &+ \mathbf{S}_3(l)\cdot\mathbf{S}_2(l+\Delta_x) \\ &+ \mathbf{S}_2(l)\cdot\mathbf{S}_1(l+\Delta_y) + \mathbf{S}_3(l)\cdot\mathbf{S}_4(l+\Delta_y)] \\ &+ J[\mathbf{S}_4(l)\cdot\mathbf{S}_2(l+\Delta_x) + \mathbf{S}_3(l)\cdot\mathbf{S}_1(l+\Delta_x) \\ &+ \mathbf{S}_3(l)\cdot\mathbf{S}_1(l+\Delta_y) + \mathbf{S}_2(l)\mathbf{S}_4(l+\Delta_y)] \\ &+ J_1[\mathbf{S}_4(l)\cdot\mathbf{S}_2(l+\Delta_{x-y}) + \mathbf{S}_3(l)\cdot\mathbf{S}_1(l+\Delta_{x+y})]\}. \end{aligned}$$

Here,

$$\begin{aligned} \Delta_x &= (b,0), \quad \Delta_y = (0,b), \\ \Delta_{x+y} &= (b,b), \quad \Delta_{x-y} = (b,-b) \end{aligned} \tag{19}$$

are the two-component vectors connecting the center of the lth plaquette to a half of the nearest neighbor plaquettes and to a half of the next-to-nearest neighbor plaquettes. The interaction between spins belonging to different plaquettes in this approximation (linear with respect to the relative deformation) is characterized by three exchange parameters (see Fig. 2):

$$I^{ex} = (1-k_1\delta)I, \quad J, \quad J_1 = (1-k_2\delta)J. \tag{20}$$

Using representations (16) and (17), the interaction operator can be written as a sum of two components,

$$H_{int} = H_{int}^\perp + H_{int}^\parallel. \tag{21}$$

Here, the transverse part of H_{int} has the following operator structure:

$$H_{int}^\perp = \frac{1}{2}\sum_{l\Delta_i}\sum_{\alpha\beta}V_{\alpha\beta}^\perp(\Delta_i)X_l^\alpha X_{l+\Delta_i}^\beta, \tag{22}$$

where the summation over Δ_i is restricted to the four vectors given by Eqs. (19). The subscripts α and β denote the so-called root vectors [11, 12] corresponding to certain transitions between the one-plaquette states $|\Phi_p\rangle$. The definition of a root vector α reduces to that of a sequence of two one-plaquette state numbers. It is assumed that the Hubbard operators X^{pq} obey the following relation: $X^{pq} \Leftrightarrow X^{\alpha(p,q)} \equiv X^\alpha$. The root vectors are 16-dimensional, which is determined by the dimension of a basis set on which the Hubbard operators are constructed. The components of a root vector α corresponding to the transition from $|\Phi_q\rangle$ to $|\Phi_p\rangle$ are defined as $\alpha_i(p, q) = \delta_{ip} - \delta_{iq}$. Introduction of the root vectors

substantially simplifies the diagram technique for the Hubbard operators [11, 12].

The sum with respect to α and β in Eq. (22) implies the summation over all the intraplaquette transitions taking place in plaquettes with the indices l and $l + \Delta_i$. For the subsequent considerations, it is important to note that the matrix elements $V^{\perp}_{\alpha\beta}(\Delta_i)$ can be represented in a form with separated indices as the scalar products

$$V^{\perp}_{\alpha\beta}(\Delta_i) = \{C^{\perp}(\alpha), \hat{V}^{\perp}(\Delta_i)C^{\perp}(-\beta)\} \tag{23}$$

of the components of an 8-vector

$$C^{\perp}(\alpha) = [\gamma^{\perp}_1(\alpha), \gamma^{\perp}_2(\alpha), \gamma^{\perp}_3(\alpha), \gamma^{\perp}_4(\alpha), \gamma^{\perp}_1(-\alpha), \gamma^{\perp}_2(-\alpha), \gamma^{\perp}_3(-\alpha), \gamma^{\perp}_4(-\alpha)] \tag{24}$$

and another 8-vector obtained upon the multiplication of the vector $C^{\perp}(-\beta)$ and the matrix $\hat{V}^{\perp}(\Delta_i)$ defined as the direct sum

$$\hat{V}^{\perp}(\Delta_i) = \hat{v}(\Delta_i) \oplus \hat{v}(\Delta_i) \tag{25}$$

of the four-row matrices $\hat{v}(\Delta_i)$ representing the parameters of interplaquette interactions

$$\hat{v}(\Delta_x) = \begin{pmatrix} 0 & 0 & 0 & 0 \\ 0 & 0 & 0 & 0 \\ J & I^{\mathrm{ex}} & 0 & 0 \\ I^{\mathrm{ex}} & J & 0 & 0 \end{pmatrix},$$

$$\hat{v}(\Delta_y) = \begin{pmatrix} 0 & 0 & 0 & 0 \\ I^{\mathrm{ex}} & 0 & 0 & J \\ J & 0 & 0 & I^{\mathrm{ex}} \\ 0 & 0 & 0 & 0 \end{pmatrix},$$

$$\hat{v}(\Delta_{x-y}) = \begin{pmatrix} 0 & 0 & 0 & 0 \\ 0 & 0 & 0 & 0 \\ 0 & 0 & 0 & 0 \\ 0 & J_1 & 0 & 0 \end{pmatrix}, \tag{26}$$

$$\hat{v}(\Delta_{x+y}) = \begin{pmatrix} 0 & 0 & 0 & 0 \\ 0 & 0 & 0 & 0 \\ J_1 & 0 & 0 & 0 \\ 0 & 0 & 0 & 0 \end{pmatrix}.$$

In a similar manner, the longitudinal part of the interaction operator can be written as

$$H^{\parallel}_{\mathrm{int}} = \sum_{l\Delta_i} \sum_{\lambda\lambda'} V^{\parallel}_{\lambda\lambda'}(\Delta_i) X^{\lambda}_{l} X^{\lambda'}_{l+\Delta_i},$$
$$V^{\parallel}_{\lambda\lambda'}(\Delta_i) = \{C^{\parallel}(\lambda), \hat{v}(\Delta_i)C^{\parallel}(\lambda')\}, \tag{27}$$

where 4-vectors $C^{\parallel}(\lambda)$ are constructed using the parameters of the S^z_i operator representation as

$$C^{\parallel}(\lambda) = [\gamma^{\parallel}_1(\lambda), \gamma^{\parallel}_2(\lambda), \gamma^{\parallel}_3(\lambda), \gamma^{\parallel}_4(\lambda)]. \tag{28}$$

It should be noted that the sum over λ in Eq. (27) for the longitudinal part of the interaction operator involves in the general case both the pairs of noncoinciding indices of one-plaquette states and the coinciding indices. This situation takes place, for example, in systems featuring a long-range order with nonzero average values of the operator S^z_i (see below). In this case, a part of the diagonal matrix elements $\langle\Phi_p|S^z_i|\Phi_p\rangle$ is nonzero, which accounts for the aforementioned feature in the longitudinal interaction.

4. DISPERSION EQUATION

In order to determine the spectrum of collective excitations of a plaquette-deformed magnet, we use a diagram technique for the Hubbard operators [11, 12] and introduce the Matsubaru Green functions:

$$D_{\alpha\beta}(f\tau; g\tau') = \langle T_\tau \tilde{X}^{\alpha}_f(\tau)\tilde{X}^{-\beta}_g(\tau')\rangle,$$
$$\tilde{X}^{\alpha}_f(\tau) = e^{\tau H} X^{\alpha}_f e^{-\tau H}. \tag{29}$$

In the loopless approximation, the Fourier image of $D_{\alpha\beta}(k, i\omega_n)$ is expressed via Green's function $G_{\alpha\beta}(k, i\omega_n)$ as [11, 12]

$$D_{\alpha\beta}(k, i\omega_n) = G_{\alpha\beta}(k, i\omega_n)b(\beta),$$

where $b(\beta)$ is the so-called terminal factor. The equation for $G_{\alpha\beta}(k, i\omega_n)$ in the graphical form appears as

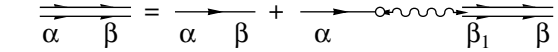

(30)

In writing this equation in an analytic form, it is important to take into account that the product of the representation parameters for the nonmagnetic phase vanishes, $\gamma^{\perp}_i(\alpha)\gamma^{\parallel}_j(\pm\alpha) = 0$, for all root vectors α and all indices i and j. This property follows from the fact that $|\Phi_q\rangle$ are the eigenstates of the operator S^z_{pl} of z-projection of the total spin moment. Since the operator S^z_j dopes not change the value of the z-projection of the

total spin moment of the plaquette, while S_i^+ increases this value by unity, the matrix elements of these operators between one-plaquette states $|\Phi_q\rangle$ cannot simultaneously differ from zero. Therefore, the collective excitations determined by the transverse and longitudinal parts of the interaction (i.e., the transverse and longitudinal oscillations) do not interact and can be determined independently.

Transverse Oscillations

Upon writing the analytic expressions corresponding to diagram (30), we obtain

$$G_{\alpha\beta}(k, i\omega_n) = \delta_{\alpha\beta}G_\alpha(i\omega_n) + \sum_{\beta_1} G_\alpha(i\omega_n)b(\alpha)V^\perp_{\alpha,\beta_1}(k)G_{\beta_1\beta}(k, i\omega_n), \tag{31}$$

where α, β, and β_1 are the root vectors corresponding to the intraplaquette transitions for which the transverse representation parameters are nonzero. The functions entering into Eq. (31) are defined as

$$G_\alpha(i\omega_n) = [i\omega_n + \alpha E]^{-1},$$
$$\alpha E = E_p - E_q, \text{ if } \alpha = \alpha(p, q),$$
$$V^\perp_{\alpha,\beta_1}(k) = \frac{1}{2}\sum_{\Delta_i}\{\exp(ik\Delta_i)V^\perp_{-\alpha,\beta_1}(\Delta_i) + \exp(-ik\Delta_i)V^\perp_{\beta_1,-\alpha}(\Delta_i)\}, \tag{32}$$

where k are the wavevectors belonging to the first Brillouin zone on a square lattice with the unit cell parameter b.

In solving system of equations (31), we will take into account the split structure (23) of the matrix elements. Introducing the 8-vector $Z_\beta(k, i\omega_n)$ with the components

$$Z^l_\beta(k, i\omega_n) = \sum_{\beta_1} C^\perp_l(\beta_1)G_{\beta_1,\beta}(k, i\omega_n), \quad l = 1, 2, \ldots, 8, \tag{33}$$

we obtain the following matrix equation for the vector components:

$$Z_\beta(k, i\omega_n) = C^\perp(\beta)G_\beta(i\omega_n) + \hat{L}^\perp(i\omega_n)\hat{M}^\perp(k)Z_\beta(k, i\omega_n). \tag{34}$$

Here, the matrix elements $\hat{L}^\perp(i\omega_n)$ are defined as

$$L^\perp_{lm}(i\omega_n) = \sum_\alpha C^\perp_l(\alpha)G^\perp_m(\alpha)G_\alpha(i\omega_n)b(\alpha), \tag{35}$$

and the matrix $\hat{M}^\perp(k)$ can be represented as

$$\hat{M}^\perp(k) = \frac{1}{2}\sum_{\Delta_i}[\exp(ik\Delta_i)\hat{V}^\perp(\Delta_i) + \exp(-ik\Delta_i)\tilde{\hat{V}}^\perp(\Delta_i)], \tag{36}$$

where $\tilde{\hat{V}}^\perp(\Delta_i)$ is the matrix transposed with respect to $\hat{V}^\perp(\Delta_i)$. Equation (34) leads to the following dispersion equation determining the spectrum of transverse excitations (upon the analytic continuation $i\omega_n \longrightarrow \omega + i\delta$, $\delta \longrightarrow +0$):

$$\det\|1 - \hat{L}^\perp(\omega)\hat{M}^\perp(k)\| = 0. \tag{37}$$

Longitudinal Oscillations

A dispersion equation for the longitudinal oscillations is derived using a procedure analogous to that outlined above for the transverse component. Omitting the details, we only present the final form of this dispersion equation:

$$\det\|1 - \hat{L}^\parallel(\omega)\hat{M}^\parallel(k)\| = 0. \tag{38}$$

Here, $\hat{L}^\parallel(\omega)$ is a 4×4 matrix with the elements defined as

$$L^\parallel_{lm}(\omega) = \sum_\alpha C^\parallel_l(\alpha)C^\parallel_m(\alpha)G_\alpha(\omega)b(\alpha), \tag{39}$$

and the matrix $\hat{M}^\parallel(k)$ can be represented as

$$\hat{M}^\parallel(k) = \sum_{\Delta_i}[\exp(ik\Delta_i)\hat{v}(\Delta_i) + \exp(-ik\Delta_i)\tilde{\hat{v}}(\Delta_i)], \tag{40}$$

where $\tilde{\hat{v}}(\Delta_i)$ is a matrix transposed with respect to $\hat{v}(\Delta_i)$.

5. THE SPECTRUM OF ELEMENTARY EXCITATIONS IN A PLAQUETTE SINGLET PHASE

Let us consider the solutions of Eqs. (37) and (38) in a low-temperature region where $T \ll I^{\text{in}}, J^{\text{in}}$. In this case, the population of the upper one-plaquette states is exponentially small:

$$N_p \le \exp(-I^{\text{in}}/T) \ll 1, \quad p = 1, 2, \ldots.$$

Therefore, the spectrum of elementary excitations is determined by the collectivization of transitions

between the ground and excited one-plaquette states. This circumstance is described by the terminal factors $b(\alpha)$ entering into $\hat{L}^{\perp}(\omega)$ and $\hat{L}^{\parallel}(\omega)$: only the $b(\alpha)$ values corresponding to the root vectors $\alpha = \alpha(p, q)$ with one argument (p or q) equal to unity do not contain exponentially small terms. In the case under consideration, there are 16 nonzero parameters $\gamma_i^{\perp}(\alpha)$ determining the elementary excitations:

$$\begin{aligned}
\gamma_1^{\perp}(1,4) &= -\gamma_2^{\perp}(1,4) = \gamma_3^{\perp}(1,4) \\
&= -\gamma_4^{\perp}(1,4) = 1/\sqrt{3}, \\
\gamma_1^{\perp}(1,8) &= \gamma_2^{\perp}(1,11) = -\gamma_3^{\perp}(1,8) \\
&= -\gamma_4^{\perp}(1,11) = -1/\sqrt{6}, \\
\gamma_1^{\perp}(2,1) &= -\gamma_2^{\perp}(2,1) = \gamma_3^{\perp}(2,1) \\
&= -\gamma_4^{\perp}(4,1) = -1/\sqrt{3}, \\
\gamma_1^{\perp}(6,1) &= \gamma_2^{\perp}(9,1) = -\gamma_3^{\perp}(6,1) \\
&= -\gamma_4^{\perp}(9,1) = 1/\sqrt{6}.
\end{aligned} \tag{41}$$

Taking into account these quantities, we conclude that the 8-dimensional $\hat{L}^{\perp}(\omega)$ matrix has a quasi-diagonal form,

$$\hat{L}^{\perp} = \hat{l}^{\perp} \oplus \hat{l}^{\perp},$$

$$\hat{l}^{\perp} = \begin{bmatrix} u+v & -u & u-v & -u \\ -u & u+v & -u & u-v \\ u-v & -u & u+v & -u \\ -u & u-v & -u & u+v \end{bmatrix}, \tag{42}$$

where u and v are defined as

$$\begin{aligned}
u &= \frac{2}{3}\frac{I^{\text{in}}}{(i\omega_n)^2 - (I^{\text{in}})^2}, \\
v &= \frac{1}{3}\frac{2I^{\text{in}} - J^{\text{in}}}{(i\omega_n)^2 - (2I^{\text{in}} - J^{\text{in}})^2}.
\end{aligned} \tag{43}$$

An analogous representation for the $\hat{M}^{\perp}(k)$ matrix as the direct sum of two matrices is

$$\hat{M}^{\perp}(k) = \hat{m}^{\perp}(k) \oplus \hat{m}^{\perp}(k),$$

$$\hat{m}^{\perp}(k) = \frac{1}{2}\begin{bmatrix} 0 & y^* I^{\text{ex}} & m_{31}^* & x^* I^{\text{ex}} \\ yI^{\text{ex}} & 0 & x^* I^{\text{ex}} & m_{42}^* \\ m_{31} & xI^{\text{ex}} & 0 & yI^{\text{ex}} \\ xI^{\text{ex}} & m_{42} & y^* I^{\text{ex}} & 0 \end{bmatrix}, \tag{44}$$

where $x = e^{ik_x a}$, $y = e^{ik_y a}$, $m_{31} = (x + y)J + xyJ_1$, and $m_{42} = (x + y^*)J + xy^*J_1$. Taking in to account that

$$\begin{aligned}
\hat{L}^{\perp}\hat{M}^{\perp} &= (l \oplus l^{\perp})(m^{\perp} \oplus m^{\perp}) \\
&= (l^{\perp}m^{\perp}) \oplus (l^{\perp}m^{\perp}),
\end{aligned} \tag{45}$$

we eventually arrive at a representation of the determinant of the eighth power via a product of two identical determinants of the fourth power. As a result, one part of the spectrum of transverse oscillations is determined from a simpler equation,

$$\det\left\|1 - \hat{l}^{\perp}(\omega)\hat{m}^{\perp}(k)\right\| = 0, \tag{46}$$

and the complete spectrum is obtained by doubling branches. This degeneracy is related to the obvious identity of the equations of motion for S_l^+ and S_l^- in the singlet phase. In the nearest-neighbor approximation, Eq. (46) can be written as

$$\begin{aligned}
&1 + 4uI^{\text{ex}}\gamma_1(k) - 2uv(I^{\text{ex}})^2[1 - \gamma_2(k)] \\
&- v^2(I^{\text{ex}})^2[1 + \gamma_2(k) - 2\gamma_3(k)] = 0,
\end{aligned} \tag{47}$$

where

$$\begin{aligned}
\gamma_l(k) &= \frac{1}{2}[\cos(lk_x b) + \cos(lk_y b)], \quad l = 1, 2, \\
\gamma_3(k) &= \cos(k_x b)\cos(k_y b).
\end{aligned}$$

Substituting the expressions for u and v into Eq. (46), we obtain a cubic equation with respect to $\omega^2(k)$ (measured in the units of $(I^{\text{in}})^2$):

$$\omega^6 + A\omega^4 + B\omega^2 + C = 0, \tag{48}$$

where

$$\begin{aligned}
A &= \frac{8}{3}\gamma_1(k)\left(\frac{I^{\text{ex}}}{I^{\text{in}}}\right) - 9, \\
B &= \frac{4}{9}[2\gamma_3(k) + 2\gamma_2(k) - 3]\left(\frac{I^{\text{ex}}}{I^{\text{in}}}\right)^2 \\
&\quad - \frac{64}{3}\gamma_1(k)\left(\frac{I^{\text{ex}}}{I^{\text{in}}}\right) + 24, \\
C &= -\frac{4}{9}[2\gamma_3(k) + 7\gamma_2(k) - 9]\left(\frac{I^{\text{ex}}}{I^{\text{in}}}\right)^2 \\
&\quad + \frac{128}{3}\gamma_1(k)\left(\frac{I^{\text{ex}}}{I^{\text{in}}}\right) - 16.
\end{aligned} \tag{49}$$

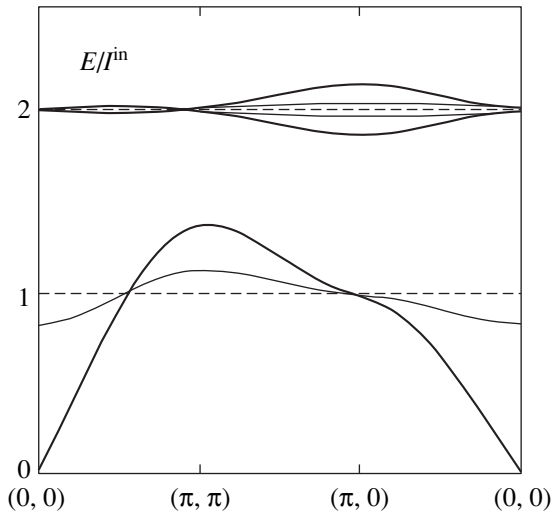

Fig. 3. Evolution of the spectrum of excitations in a plaquette singlet phase with increasing I^{ex}/I^{in} ratio (see text for explanations).

Solving the cubic equation (48), we determine three branches of the spectrum of collective excitations:

$$\omega_1^2 = -\frac{1}{3}A + \frac{1}{6}W - \frac{2Z}{W},$$

$$\omega_2^2 = -\frac{1}{3}A - \frac{1}{12}W + \frac{Z}{W} + i\frac{\sqrt{3}}{2}\left(\frac{W}{6} + \frac{2Z}{W}\right), \qquad (50)$$

$$\omega_3^2 = -\frac{1}{3}A - \frac{1}{12}W + \frac{Z}{W} - i\frac{\sqrt{3}}{2}\left(\frac{W}{6} + \frac{2Z}{W}\right),$$

where

$$W = \{36BA - 108C - 8A^3 + 12(12B^3$$

$$-3B^2A^2 - 54BAC + 81C^2 + 12CA^3)^{1/2}\}^{1/3}, \qquad (51)$$

$$Z = B - \frac{1}{3}A^2.$$

The other three branches are determined from an analysis of the dispersion equation for the longitudinal oscillations. Since the operators S_f^x, S_f^y, and S_f^z in the singlet phase are equivalent, the dynamics generated by these operators are identical. Therefore, nonzero representation parameters $\gamma^{\parallel}(\alpha)$ connect the same one-plaquette states as parameters $\gamma^{\perp}(\alpha)$.

As a result, the dispersion equation in this case is identical to Eq. (46). This provides another three branches of the low-temperature spectrum. Thus, the complete spectrum of excitations in a plaquette singlet phase at $T \ll I^{in}$ exhibits three triply degenerate branches.

Figure 3 shows the pattern of evolution of the spectrum of excitations (the triple degeneracy of branches is not depicted) in a plaquette singlet phase with increasing I^{ex}/I^{in} ratio. At $I^{ex} = 0$, where all plaquettes are independent, the spectrum exhibits one branch with the energy I^{in} and two degenerate branches with the energies $2I^{in}$ (depicted by dashed curves in Fig. 3). At a finite but small I^{ex}/I^{in} ratio, a dispersion appears that leads to splitting of the upper branches. Thin solid curves in Fig. 3 show the spectrum for $I^{ex}/I^{in} = 1/9$, and thick solid curves, for the limiting case of $I^{ex}/I^{in} = 3/8$. In the latter case, the lower branch becomes activationless. For $I^{ex}/I^{in} > 3/8$, the spectrum loses positive definiteness (ω_2^2 becomes negative), which corresponds to the transition to a state with long-range AFM ordering.

The inclusion of the frustrated-spin-type interactions involving the next-to-nearest neighbor spin moments leads to the stabilization of a nonmagnetic phase. The corresponding analytic expressions are not presented here for being rather lengthy. It should be noted that the instability also primarily appears at $\mathbf{k} = (0, 0)$, where the ω_2 value is given by the formula

$$\omega_2^2(\mathbf{k} = 0) = \frac{4}{3}I^{in}\left(2J - 2I^{ex} + \frac{3}{4}I^{in} + J_1\right). \qquad (52)$$

The condition of positive definiteness of the spectrum yields the following boundary of stability of a plaquette singlet phase:

$$\left(\frac{J}{I}\right)_c = \frac{5 - 11(k_1\delta)}{12 - 4(k_2\delta)}. \qquad (53)$$

The stable plaquette singlet phase is formed at $J/I > (J/I)_c$. With neglect of the deformation, the plaquette singlet phase is formed at $J > 5I/12$. In the absence of frustrated spin interactions, a transition from the plaquette singlet phase will take place at $k\delta = 5/11$ that corresponds to $I^{ex}/I^{in} = 3/8$.

In the region of $J/I < (J/I)_c$, a plaquette singlet phase does not correspond to the ground state of the system. In this case, the system exhibits spontaneous symmetry-breaking with the formation of a long-range AFM order and an additional deformation of the lattice. In order to describe such a state, it is necessary to modify the plaquette representation and take into account the influence of the magnetic structure on the basis set functions describing the one-plaquette states. Here, a necessary criterion of the correct description of the magnetic phase is the existence of a Goldstone boson in the system. This situation is considered in the next section.

6. PLAQUETTE REPRESENTATION WITH ALLOWANCE FOR SELF-CONSISTENT FIELD

In order to take into account the possible AFM order in the 2D spin system, let us modify the scheme of construction of the plaquette representation so as to include the ordering effects. The order parameter must be determined either from the condition of minimization of the system energy or from the solution of the self-consistent equation.

The appearance of a long-range AFM order results in a self-consistent field beginning to act on each spin plaquette. Assuming that the ground state of the system has the Néel character, for certainty we will set

$$\langle S_1^z(l)\rangle = -\langle S_2^z(l)\rangle = \langle S_3^z(l)\rangle = -\langle S_4^z(l)\rangle = \sigma. \quad (54)$$

Using the well-known procedure of self-consistent field introduction (in the diagram form of perturbation theory, this corresponds to the exact allowance for all one-tail diagrams [15]), the rule of modification of the unperturbed Hamiltonian H_0 can be written as

$$H_0 \longrightarrow \tilde{H}_0 = \sum_l \tilde{h}_0(\sigma; l) = \sum_l \{2\bar{H}\sigma - \bar{H}D^z(l) + h_0(l)\}, \quad (55)$$

where $\bar{H} = (2I^{ex} - 2J - J_1)\sigma$ is the self-consistent field and $D^z(l)$ is the AFM ordering operator that acts on the plaquette spin moments as described by the relation

$$D^z(l) = S_1^z(l) - S_2^z(l) + S_3^z(l) - S_4^z(l). \quad (56)$$

The renormalized eigenfunctions of a one-plaquette Hamiltonian, which satisfy the Schrödinger equation (the plaquette index is omitted)

$$\tilde{h}_0(\sigma)|\tilde{\Phi}_p(\sigma)\rangle = E_p(\sigma)|\tilde{\Phi}_p(\sigma)\rangle, \quad (57)$$

can be found in the form of a superposition of the unmodified one-plaquette states:

$$|\tilde{\Phi}_p(\sigma)\rangle = \sum_{n=1}^{16} C_{pn}(\sigma)|\Phi_n\rangle. \quad (58)$$

The eigenfunctions of a separate plaquette upon modification depend not only on I^{in} and J^{in}, but also on the interplaquette interaction parameters I^{ex}, J, and J_1. The self-consistent equation for equilibrium magnetization is

$$\sigma = \frac{1}{4}\langle\tilde{\Phi}_1(\sigma)|\hat{D}^z|\tilde{\Phi}_1(\sigma)\rangle, \quad (59)$$

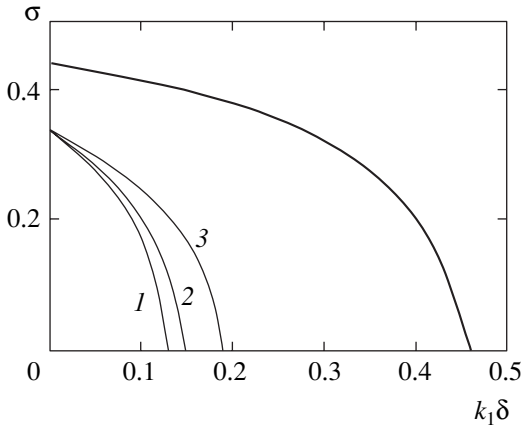

Fig. 4. Plots of the magnetization of the AFM sublattice versus plaquette deformation parameter $k_1\delta$ for nonfrustrated (thick solid curve) and frustrated ($J/I = 0.3$) antiferromagnets for three values of the relative rate of decrease in the exchange integrals: $k_2/k_1 = 0$ (*1*), 1 (*2*) and 3 (*3*).

where $|\tilde{\Phi}_1(\sigma)\rangle$ is the ground-state function of a plaquette occurring in the self-consistent field. The system energy per plaquette is given by the formula

$$E(\sigma) = \langle\tilde{\Phi}_1(\sigma)|\tilde{h}_0(\sigma)|\tilde{\Phi}_1(\sigma)\rangle. \quad (60)$$

As is known [13, 14], the frustrated spin interactions tend to suppress the long-range AFM ordering. In the simplest approximation, the point of breakage of the magnetic order corresponds to the critical exchange parameter $J_c = I/2$. In the case under consideration, the solution to the self-consistent equation (59) shows that a state with spontaneously violated symmetry exists only in the region of $J < \tilde{J}_c = 0.417I$. Thus, allowance for the intraplaquette quantum fluctuations led to a shift of the transition point toward lower J values.

The appearance of plaquette deformation in the lattice induces an additional mechanism of spontaneous violation of magnetization order with the subsequent transition of the spin ensemble to a singlet state. This mechanism is related to a different change in the intra- and interplaquette exchange integrals upon plaquette deformation. Figure 4 shows a decrease in the sublattice magnetization as a result of the plaquette deformation of nonfrustrated (thick solid curve) and frustrated ($J/I = 0.3$) antiferromagnets for three values of the relative rate of decrease in the exchange integrals: $k_2/k_1 =$ 0 (*1*), 1 (*2*) and 3 (*3*). As can be seen, the critical values of relative deformation significantly depend on the k_2/k_1 ratio and decrease with increasing rate of frustrated spin interactions.

It should be noted that the magnetization corresponds to a minimum in the dependence of the system energy on σ. In the nonfrustrated case, the energy per plaquette is $E_{min} = -2.336I$. A decrease in the ground

state energy as compared to that ($E_{\text{Neel}} = -2I$) of the Néel phase in the usual description is also caused by taking into account the nearest quantum fluctuations.

Allowance for the self-consistent field in the presence of a long-range AFM order does not change the form of the transverse interaction term ($H_{\text{int}}^{\perp}$), but modifies the longitudinal interaction component ($H_{\text{int}}^{\parallel}$). This is related to the fact that a nonzero magnetization of the sublattice leads to nonzero longitudinal representation parameters $\gamma_i^{\parallel}(\alpha)$. As a result, the terms with coinciding indices must be taken into account in summing over the pair indices of one-plaquette states. The renormalization of a zero-order Hamiltonian related to the inclusion of the self-consistent field effects involves replacement of the diagonal Hubbard operators in $H_{\text{int}}^{\parallel}$ according to the following rule: $X_f^{nn} \longrightarrow \Delta X_f^{nn} = X_f^{nn} - \langle X_f^{nn} \rangle$ [11, 15].

7. SPECTRUM OF EXCITATIONS IN THE MAGNETIC PHASE AND THE ENERGY OF ZERO-POINT OSCILLATIONS

In order to determine the spectrum of elementary excitations and corrections to the energy due to the zero-point quantum oscillations in the phase with spontaneous symmetry-breaking and plaquette deformation, let us use the above representation for the magnetic phase and restrict consideration to the low-temperature case. Then, the spectral problem is conveniently solved using a Bose analog of the Hamiltonian. The strict theory of construction of the Bose Hamiltonian analog with recourse to an indefinite metric is presented in [16, 17].

In the case under consideration, the interaction between quasi-particles is ignored and the passage to the Bose Hamiltonian analog is provided by replacing the Hubbard operators with the Bose operators according to the following scheme:

$$X_l^{1,\,p+1} \longrightarrow b_p(l), \quad X_l^{p+1,\,1} \longrightarrow b_p^+(l), \qquad p = 1, 2, \ldots, 15, \tag{61}$$

where $b_p(l)$ ($b_p^+(l)$) is the p-type boson annihilation (creation) operator in the plaquette representation. The Bose operators $X_l^{p+1,\,q+1}$ for $p \neq 0$, $q \neq 0$ contain at least the product of two operators, $X_l^{p+1,\,q+1} \longrightarrow b_p^+(l)b_q(l)$ and, hence, the Hamiltonian terms with such operators describe the interaction between quasiparticles. Therefore, a quadratic form of the Hamiltonian can be obtained by retaining in the sums over the root vectors α and β only the terms corresponding to the transitions between one-plaquette states, one of which is the plaquette ground state.

Taking into account the above considerations, a quadratic form of the Hamiltonian can be written as

$$\begin{aligned} H_{\text{int}}^{\perp} = \frac{1}{2}\sum_{l\Delta_i}\sum_{p,\,q=1}^{15} \{ & V_{1,\,p+1;\,1,\,q+1}^{\perp}(\Delta_i) b_p(l) b_q(l+\Delta_i) \\ & + V_{p+1,\,1;\,1,\,q+1}^{\perp}(\Delta_i) b_p^+(l) b_q(l+\Delta_i) \\ & + V_{1,\,p+1;\,q+1,\,1}^{\perp}(\Delta_i) b_p(l) b_q^+(l+\Delta_i) \\ & + V_{p+1,\,1;\,q+1,\,1}^{\perp}(\Delta_i) b_p^+(l) b_q^+(l+\Delta_i) \}, \end{aligned} \tag{62}$$

where $V_{1,\,p+1;\,q+1,\,1}^{\perp}(\Delta_i)$ denotes the matrix element $V_{\alpha\beta}^{\perp}(\Delta_i)$ introduced above with $\alpha = \alpha(1, p+1)$ and $\beta = \beta(q+1, 1)$. Analogous notations are used for the other matrix elements in expression (62). In the momentum representation, this quadratic form appears as

$$\begin{aligned} H_{\text{int}}^{\perp} = \sum_k \sum_{p,\,q\neq 1} \Big\{ & \frac{1}{2} R_{pq}(k) b_p^+(k) b_q^+(-k) \\ & + S_{pq}(k) b_p^+(k) b_q(k) \\ & + \frac{1}{2} R_{pq}^*(k) b_p(k) b_q(-k) \Big\}, \end{aligned} \tag{63}$$

where

$$\begin{aligned} R_{pq}(k) &= \frac{1}{2}\sum_{\Delta_i} \{ V_{1,\,p+1;\,1,\,q+1}^{\perp}(\Delta_i) \exp(ik\Delta_i) \\ &\quad + V_{1,\,q+1;\,1,\,p+1}^{\perp}(\Delta_i) \exp(-ik\Delta_i) \}, \\ S_{pq}(k) &= \frac{1}{2}\sum_{\Delta_i} \{ V_{p+1,\,1;\,1,\,q+1}^{\perp}(\Delta_i) \exp(ik\Delta_i) \\ &\quad + V_{q+1,\,1;\,1,\,p+1}^{\perp}(\Delta_i) \exp(-ik\Delta_i) \}. \end{aligned} \tag{64}$$

The complete Hamiltonian describing the spectrum of transverse oscillations has the usual structure, $H^{\perp} = H_0^{\perp} + H_{\text{int}}^{\perp}$, where the energy operator of noninteracting one-plaquette bosons is given by the following expression:

$$H_0 = \sum_k {\sum_p}' E_{p+1} b_p^+(k) b_p(k). \tag{65}$$

Here, the primed sum with respect to p is taken over the indices for which the representation parameters of spin

operators $\gamma_i^{\perp}(1, p+1)$ and $\gamma_i^{\perp}(p+1, 1)$ for $i = 1, 2, 3, 4$ are nonzero.

In order to calculate the energy spectrum and the contribution of zero-point oscillations to the ground state energy, let us perform a unitary transformation of the Hamiltonian as [18]

$$b_p(k) = \sum_r u_{pr}(k)a_r(k) + \sum_r v^*_{pr}(-k)a^+_r(-k). \quad (66)$$

The problem of diagonalization reduces to the algebraic problem of determining eigenvalues,

$$\begin{aligned}\sum_s \tilde{S}_{ps}(k)u_{sr}(k) + \sum_s R_{ps}(k)v_{sr}(k) &= E_r(k)u_{pr}(k),\\ -\sum_s R_{ps}(-k)u_{sr}(k) - \sum_s \tilde{S}_{ps}(k)v_{sr}(k) &= E_r(k)v_{pr}(k),\end{aligned} \quad (67)$$

where

$$\tilde{S}_{ps} = S_{ps} + \delta_{ps}(E_{p+1} - E_1). \quad (68)$$

With the new operators, the Hamiltonian acquires the following form:

$$H = \Delta E_0 + \sum_{k,\nu} E_\nu(k)a^+_\nu(k)a_\nu(k), \quad (69)$$

where the quantum additive to the ground-state energy is determined as

$$\Delta E_0 = -\sum_{\nu,k}\left\{\sum_p |v_{p\nu}(k)|^2\right\}E_\nu(k). \quad (70)$$

A similar procedure is used to calculate the spectrum of longitudinal oscillations. A quadratic form of the Hamiltonian for this case can be obtained from expression (63) by replacing $V^{\perp}_{\alpha,\beta} \longrightarrow V^{\parallel}_{\alpha,\beta}$ and eliminating the factor 1/2. The resulting quadratic form of the complete Hamiltonian is a direct sum of two independently diagonalized quadratic forms.

Figure 5 shows the results of numerical calculations of the low-energy part of the spectrum of oscillations in the magnetic phase for three values of the plaquette deformation parameters. For simplicity, we restricted the consideration to the case of $J = 0$. In the case of $J \neq 0$, the character of evolution of the spectrum of elementary excitation is qualitatively similar. At the point of transition, where $k_1\delta = 0.45$, the spectrum exhibits threefold degeneracy (two transverse branches and one longitudinal branch) that exactly corresponds to the solution obtained previously using a cubic equation (curve *1*).

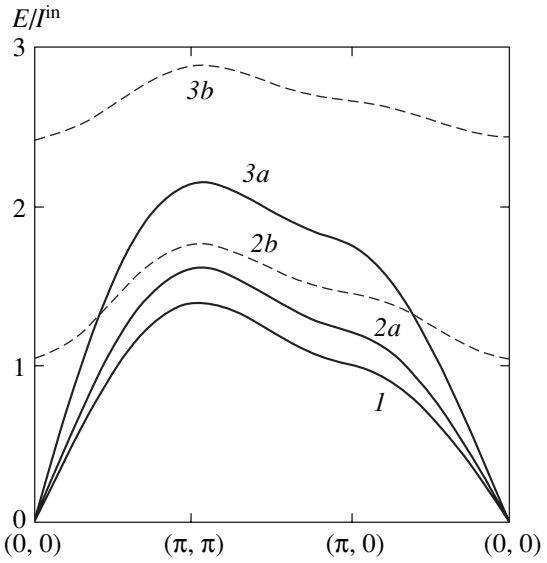

Fig. 5. The results of numerical calculations illustrating the evolution of the low-energy part of the spectrum of oscillations in the AFM phase (see the text for explanations).

A decrease in the degree of plaquette deformation in the AFM phase leads to removal of the threefold degeneracy, whereby the two branches of transverse oscillations retain the Goldstone character and the longitudinal branch (dashed curve in Fig. 5) exhibits the activation character. For $k_1\delta = 0.3$, the transverse and longitudinal branches are depicted by curves *2a* and *2b*; the limiting case of nondeformed antiferromagnet is illustrated by curves *3a* and *3b*.

The obtained data concerning the evolution of the spectrum of oscillations show that an acoustic boson exists (in accordance with the Goldstone theorem) in the presence of plaquette deformation unless the long-range AFM order is broken. On approaching the point of a transition to the singlet phase, the longitudinal (optical) mode exhibits softening. At the transition point and in the singlet phase, the energy spectra of the transverse and longitudinal oscillations fully coincide. An increase in the degree of plaquette deformation in the singlet phase leads to the appearance of an activation energy. Thus, the oscillation spectrum in the singlet phase is gapped and threefold degenerate. The gap width grows with increasing stability of the singlet phase, that is, with the system moving away from the transition point.

In order to determine the equilibrium value of the parameter of plaquette deformation δ and to construct the phase diagram of a 2D quantum magnet with frustrated spin coupling, let us take into account the energy contribution related to the lattice distortion. In the case under consideration, this deformation energy per

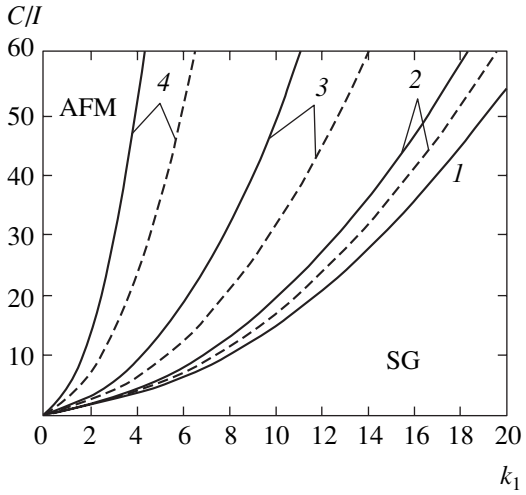

Fig. 6. The phase diagram of a frustrated plaquette-deformed 2D quantum magnet (see text for explanations).

plaquette can be written as $E_{el} = 2C\delta^2$, where C/a_0^2 is the effective constant of elastic interaction. Then, the equilibrium relative deformation δ is determined from the equation

$$\frac{\partial E_m(\delta)}{\partial \delta} + 4Ca_0^2\delta = 0, \tag{71}$$

where E_m is the magnetic energy of the spin system. At the point of the transition to the singlet phase, the parameter δ is not only a solution to Eq. (71), but also corresponds to the critical product $(k_1\delta)_c$. The two conditions are met provided that

$$C = \mu k_1^2. \tag{72}$$

This relation determines the boundary between the AFM and plaquette singlet phases. The coefficient μ is given by the formula

$$\mu = -\frac{1}{4(k_1\delta)_c}\left(\frac{\partial E_m}{\partial(k_1\delta)}\right)_{k_1\delta = (k_1\delta)_c} \tag{73}$$

and depends on the model parameters J/I and k_2/k_1.

Figure 6 presents the phase diagram of a frustrated plaquette-deformed 2D quantum magnet, where curve *1* shows the phase boundary for the nonfrustrated quantum magnet. The pairs of curves *2–4* represent the lines of the phase transitions in the frustrated quantum magnets with $J/I = 0.1$, 0.3, and 0.4, respectively, where solid lines refer to the case of $k_2 = 0$ (whereby the dependence of the exchange integral on the distance is ignored) and dashed lines, to $k_2/k_1 = 1$ (equal relative rates of variation of the exchange parameters I and J). This phase diagram quantitatively illustrates that small k_1 values (indicative of the exchange integrals slowly varying with deformation) and large elastic constants C correspond to a quantum magnet with plaquette-deformed AFM phase and renormalized sublattice magnetization in the ground state. As k_1 increases and/or C decreases, the quantum magnet exhibits a second-order phase transition from the AFM to the singlet phase.

8. CONCLUSIONS

The results presented in this paper show that the inclusion of MEC effects in a 2D spin system on a square lattice can be a decisive factor in the mechanism of a singlet ground state formation with a gapped spectrum of elementary excitations. It should be emphasized that it is the MEC that introduces a difference between the intra- and interplaquette exchange interactions and thus accounts for the appearance of a branch with the activation character in the spectrum. Although frustrated spin interactions break the long-range AFM order, these interactions alone are insufficient for eliminating the gapless excitations.

The second important issue is the choice of the type of lattice deformation. The consideration was restricted to the case of plaquette deformation for two reasons. First, the square lattice symmetry to a certain extent instigates this type of deformation. Second, the energy factors rendering the plaquette singlet state preferable also justify the adopted scenario of "singletization" of a 2D quantum magnet with MEC. Using the Hubbard operator technique within the framework of the developed plaquette representation, it is possible to completely take into account the strong one-plaquette correlations and thus correctly describe the tendency toward a second-order phase transition from the AFM to the singlet phase in a plaquette-deformed quantum magnet.

The third important point in the proposed theory consists in that the excitation spectrum has been calculated using the complete (rather than truncated) set of one-plaquette states. Only this approach leads to the excitation spectrum satisfying the necessary symmetry conditions. In particular, a Goldstone boson exists in the phase with spontaneously broken symmetry in accordance with the Goldstone theorem. In this context, it should be recalled that this boson exists provided that not only the first (lowest) excited one-plaquette states, but also the highest states of the plaquette quintet, are taken into consideration.

To summarize, a model has been proposed that describes the phase transition on a square spin lattice from the AFM to the singlet state with respect to the MEC parameter. The spectrum of elementary excitations in both singlet and AFM phases was calculated within the framework of the common approach. In particular, It is established that the transition from the AFM to singlet phase is related to softening of the lon-

gitudinal branch of oscillations. In the singlet phase, the spectral gap plays the role of a parameter characterizing the distance to the phase transition point.

ACKNOWLEDGMENTS

The authors are grateful to V.I. Zinenko for fruitful discussions of the results.

This study was supported by the Krasnoyarsk Regional Science Foundation and the Russian Foundation for Basic Research (joint project no. 05-02-97710) and by the Presidium of the Russian Academy of Sciences (within the framework of the "Quantum Macrophysics" program).

REFERENCES

1. G. A. Petrakovskiĭ, K. A. Sablina, A. M. Vorotynov, *et al.*, Zh. Éksp. Teor. Fiz. **98**, 1382 (1990) [Sov. Phys. JETP **71**, 772 (1990)].
2. M. Hase, I. Terasaki, and K. Uchinokura, Phys. Rev. Lett. **70**, 3651 (1993).
3. N. Katoh and M. Imada, J. Phys. Soc. Jpn. **64**, 4105 (1995).
4. H. Kageyama, K. Yoshimura, R. Sterm, *et al.*, Phys. Rev. Lett. **82**, 3168 (1999).
5. M. B. Stone, I. Zaliznyak, D. H. Reich, *et al.*, Phys. Rev. B **64**, 144405 (2001).
6. L. N. Bulaevskiĭ, Zh. Éksp. Teor. Fiz. **44**, 1008 (1963) [Sov. Phys. JETP **17**, 684 (1963)].
7. G. A. Petrakovskiĭ, K. A. Sablina, A. M. Vorotynov, *et al.*, Fiz. Tverd. Tela (St. Petersburg) **41**, 677 (1999) [Phys. Solid State **41**, 610 (1999)].
8. H. Sakurai, N. Tsuboi, M. Kato, *et al.*, Phys. Rev. B **66**, 024428 (2002).
9. A. F. Barabanov, L. A. Maksimov, O. A. Starykh, *et al.*, J. Phys.: Condens. Matter **2**, 8925 (1990).
10. S. V. Vonsovskiĭ, *Magnetism* (Nauka, Moscow, 1971; Wiley, New York, 1974), p. 1032.
11. R. O. Zaitsev, Zh. Éksp. Teor. Fiz. **68**, 207 (1975) [Sov. Phys. JETP **41**, 100 (1975)].
12. R. O. Zaitsev, Zh. Éksp. Teor. Fiz. **70**, 1100 (1976) [Sov. Phys. JETP **43**, 574 (1976)].
13. A. Chubukov, Phys. Rev. B **44**, 392 (1991).
14. A. Chubukov, S. Suchdev, and J. Ye, Phys. Rev. B **49**, 11919 (1994).
15. Yu. A. Izyumov, F. A. Kassan-ogly, and Yu. N. Skryabin, *Field Methods in the Theory of Ferromagnetism* (Nauka, Moscow, 1974), p. 224 [in Russian].
16. V. V. Val'kov and T. A. Val'kova, Pis'ma Zh. Éksp. Teor. Fiz. **52**, 1179 (1991) [JETP Lett. **52**, 589 (1991)].
17. V. V. Val'kov and T. A. Val'kova, Zh. Éksp. Teor. Fiz. **99**, 1881 (1991) [Sov. Phys. JETP **72**, 1053 (1991)].
18. S. V. Tyablikov, *Methods in the Quantum Theory of Magnetism* (Nauka, Moscow, 1975), p. 528.

Translated by P. Pozdeev